



OPEN ACCESS

EDITED BY

Pradeep R. Varadwaj,
The University of Tokyo, Japan

REVIEWED BY

Sani Amril Samsudin,
University of Technology Malaysia, Malaysia
Ritima Banerjee,
Calcutta Institute of Technology, India

*CORRESPONDENCE

Azizeh Javadi,
✉ ajavadi@aut.ac.ir

RECEIVED 27 January 2024

ACCEPTED 05 March 2024

PUBLISHED 21 March 2024

CITATION

Negaresh M, Javadi A and Garmabi H (2024),
Poly(lactic acid)/ poly(ϵ -caprolactone) blends:
the effect of nanocalcium carbonate and
glycidyl methacrylate on interfacial
characteristics.
Front. Mater. 11:1377340.
doi: 10.3389/fmats.2024.1377340

COPYRIGHT

© 2024 Negaresh, Javadi and Garmabi. This is
an open-access article distributed under the
terms of the [Creative Commons Attribution
License \(CC BY\)](https://creativecommons.org/licenses/by/4.0/). The use, distribution or
reproduction in other forums is permitted,
provided the original author(s) and the
copyright owner(s) are credited and that the
original publication in this journal is cited, in
accordance with accepted academic practice.
No use, distribution or reproduction is
permitted which does not comply with
these terms.

Poly(lactic acid)/ poly(ϵ -caprolactone) blends: the effect of nanocalcium carbonate and glycidyl methacrylate on interfacial characteristics

Mohammadmahdi Negaresh, Azizeh Javadi* and
Hamid Garmabi

Department of Polymer Engineering and Color Technology, Amirkabir University of Technology,
Tehran, Iran

To expand the potential applications of polylactic acid (PLA), it is essential to incorporate a highly flexible polymer into the blend. Polycaprolactone (PCL) is an ideal choice due to its ductility and biodegradability. However, blending PLA with PCL resulted in weak mechanical properties. To address this issue, glycidyl methacrylate (GMA) and nano calcium carbonate (NCC) were introduced to enhance the adhesion at the interface between PLA and PCL. SEM images provided clear visual evidence of the impact of GMA and NCC on the morphology of the blend. Both components were effective in reducing the size of the dispersed PCL phase, shrinking it to approximately half the size of the original blend. Spectroscopic analysis revealed that GMA caused a reaction between its epoxy group and the hydroxyl and carboxyl groups of PLA and PCL. This reaction led to the formation of strong peaks in the 6.5 to 7.5 range in ^1H NMR, as well as peaks at 76 and 139 ppm in ^{13}C NMR. These findings were further corroborated by FT-IR, which demonstrated that NCC, despite its surface coating, did not create any new bonds. Rheological studies further demonstrated the positive effects of GMA and NCC. Both the storage modulus (G') and complex viscosity (η^*) of the blends increased, showing improved post-processing performance. Investigation into the shear-thinning behavior of the uncompatibilized blends revealed that NCC caused a significant decrease in complex viscosity at higher frequencies, indicating the disruption of the nanoparticle network. The power-law slope was measured to be 0.62. In contrast, the blend containing the compatibilizer demonstrated a moderate decrease in viscosity, with a power-law slope of 0.36. To analyze the behavior of the PLA/PCL blends in the presence of compatibilizers and nanoparticles at intermediate frequencies, the Palirene model was utilized. The superior integrity of the compatibilized blend was effectively demonstrated by the model, which showed enhanced stress transfer and phase relaxation.

KEYWORDS

polylactic acid, polycaprolactone, compatibilizer, nanoparticle, interfacial tension

1 Introduction

Over the past few decades, the excessive use of nonbiodegradable polyolefin-based plastics has caused significant environmental issues, including increased waste generation and the accumulation of commercial and industrial waste in landfills (Huang et al., 2022; Agarwal, 2020). In an effort to address this problem, numerous attempts have been made to replace non-degradable polymers with biodegradable alternatives (Huneault and Li, 2012; Pilla et al., 2009). One such polymer that has garnered attention is poly(lactic acid) (PLA) due to its desirable properties such as excellent gloss and clarity, high tensile strength, good processability, and low coefficient of friction (Huda et al., 2005; Farah et al., 2016). These properties make PLA well-suited for various medical and packaging applications (Lim et al., 2008). However, the brittleness of PLA limits its use to specific applications, and PLA also exhibits slow crystallization kinetics (De Santis et al., 2011; Gao et al., 2023). To overcome these drawbacks, much research has been focused on modifying PLA through methods such as blending with other polymers and filling with inorganic particles (Dorgan et al., 1999; Palade et al., 2001; Zhou et al., 2007).

The effect of nanoparticles on the compatibility level of polymer blends refers to the ability of nanoparticles to enhance the compatibility and interaction between two polymers that would be either incompatible or have poor mixing behavior. When two polymers with different chemical structures or polarities are blended, they typically exhibit phase separation, leading to the formation of distinct domains or phases within the blend. This phase separation can result in poor mechanical properties and limited functionality for many applications (Banerjee and Ray, 2021). Nanoparticles, particularly those that are surface-modified or functionalized, can act as a compatibilizer in polymer blends. These nanoparticles are designed to have affinity for both polymers in the blend, acting as bridges or mediators between the two phases, promoting their compatibility. The compatibilizing effect of nanoparticles can be attributed to several mechanisms (Ye et al., 2022). Firstly, steric stabilization is a notable effect in which nanoparticles with specific surface modification (e.g., polymer brushes) form a layer around the nanoparticles, reducing interfacial tension and preventing phase separation. Secondly, nanoparticles can create strong adhesion at the interface between the two polymer phases, improving the interfacial strength and preventing phase separation. Moreover, nanoparticles can act as physical barriers hindering chain motion and promoting interdiffusion between polymer chains. This can lead to the formation of a more uniform and mixed structure, enhancing compatibility. Finally, nanoparticles serve as nucleating agents, enhancing the dispersion of one polymer phase within the other and reducing the size of phase-separated domains (in the sea-island morphology).

In addition, inorganic particles are commonly used to enhance the strength of polymers (Oksman et al., 2006; Najafi et al., 2013; Sabzi et al., 2013). The research conducted by Lu et al. (Özen Öner et al., 2022) successfully showed that the incorporation of rare Earth oxide nanoparticles at the interface of PLA and PCL resulted in a significant increase in crystallinity of the blend. Consequently, overall entropy of the polymer blend decreased by reducing chain mobility. Additionally, intermolecular interactions

between polymer chains at the interface made considerable improvement in both mechanical properties and thermal stability.

One of the most common nanoparticles is nanosized calcium carbonate (NCC), which is widely employed in rubbers, plastics, and paints due to its cost-effectiveness. NCC can improve PLA's thermal and processing properties while also reducing costs (Koivula et al., 2012; Liang et al., 2015; Cheng et al., 2020). Mechanical properties, including tensile properties, impact strength, and flexural properties, are crucial indicators of material performance (Zhai et al., 2021). In a study conducted by Liang et al. (2015), the addition of NCC to PLA resulted in an increase in the elastic modulus but a decrease in tensile strength and elongation at break. Moreover, an increase in NCC content from 1 to 4 wt.% led to a linear increase in the elastic modulus of 52%. However, the non-linear decrease in tensile strength and elongation at break was limited to 12% and 19% respectively.

One approach to improve the unfavorable properties of PLA, such as brittleness, is to blend PLA with ductile polymers (Bhatia et al., 2007; Al-ityry et al., 2014; Arrieta et al., 2017). Blending can significantly impact the resulting mechanical properties, which depend on the mechanical properties of the components, blend microstructure, and the interface between phases (Chuaonpat et al., 2020; Chen et al., 2023). However, one challenge in formulating new polymeric blends is predicting how additives will influence the overall phase behavior and performance, especially when the blend involves incompatible polymers with weak interfacial adhesion and hence poor mechanical properties (Qader et al., 2022; Guo et al., 2019). To enhance interfacial adhesion between the phases and reduce interfacial tension, the use of suitable compatibilizers is appropriate. Compatibilizers are typically macromolecules, such as block copolymers, which manipulate interfacial properties (Standau et al., 2019; Torres et al., 2021).

In contrast to PLA, poly(ϵ -caprolactone) (PCL) offers high flexibility, but has relatively low strength and a low melting point of 60°C, which restricts its use to certain applications. Therefore, blending PLA with PCL has the potential to improve flexibility or increase strength compared to each individual component (Matumba et al., 2023; Fortelny et al., 2019). In recent years, blends of PLA with more flexible biodegradable polymers, such as PCL, have been explored and developed (Ferrer et al., 2021; Todo and Takayam, 2011). Although these blends may not exhibit desired properties due to their incompatibility, several interesting results have been observed (Semba et al., 2006; Harada et al., 2008; Jha et al., 2019).

Various compatibilizers, such as PLA-co-PCL, have been investigated to improve the compatibility of PLA/PCL blends and enhance their mechanical properties, such as impact strength (Maglio et al., 2004). Harada et al. (2008) demonstrated that lysine triisocyanate (LTI) was more effective as a reactive processing agent for PLA/PCL blends compared to lysine diisocyanate (LDI) and other isocyanates. However, LTI is not suitable for biocompatibility.

Glycidyl methacrylate (GMA) is a suitable material for enhancing the interfacial adhesion between components in blends. The epoxy groups in GMA can react with the carboxyl or hydroxyl groups of polyesters (Chee et al., 2013). Therefore, toughness is a result of better interfacial adhesion. In another study, an ethylene-methyl acrylate-glycidyl methacrylate terpolymer was employed to

reduce interfacial tension between PLA and PCL. The incorporation of 8 phr of compatibilizer through melt blending in PLA/PCL (90/10) achieved the expected toughening effect, leading to a notch impact strength of 64.31 kJ/m². Recently, researchers have successfully used a glycidyl methacrylate PLA compatibilizer to improve the compatibility of PLA/PCL blends. This approach resulted in higher thermal stability, a lower melting point, and an elongation at break 60 times greater than that of PLA/PCL without compatibilizer (Ye et al., 2023).

Improvement in compatibility of PLA/PCL blend can lead to exclusive applications, such as in packaging materials, medical devices, and drug delivery systems. This current study aimed to demonstrate that even though there have been preconceived notions about the effectiveness of multi-functional compatibilizers or nanoparticles with specific surface modifications in enhancing the compatibility of polymer blends, using traditional single-factor compatibilizers or nanoparticles with simple surface modification can still lead to improvement in the blends mechanical and other properties. Additionally, a careful consideration of other aspects such as molecular weight, morphology, and rheology in the polymer system can achieve a suitable balance in the conclusion of the effect of these two types of additives. Moreover, rheological test results were used to evaluate behaviors of two polymers at their interface using the Palierne model before and after compatibilizing. Therefore, the objective of this study is to investigate the individual effects of the GMA compatibilizer and NCC nanoparticle on the properties of PLA/PCL blend.

2 Experimental

2.1 Materials

Poly (lactic acid) (PLA) with a grade of 2003D, obtained from Nature Works, USA, has a melt flow rate of 6 g/10 min (190°C/2.16 kg) and a density of 1.24 g/cm³. The Poly (ϵ -caprolactone) (PCL) used is CapaTM6800, purchased from Perstorp, Sweden, with a melt flow rate of 4 g/10 min (160°C/5 kg) and a density of 1.13 g/cm³. Glycidyl methacrylate (GMA), obtained from Alfa Aesar, Germany, has a density of 1.08 g/cm³ and a boiling point of 189°C. Nano calcium carbonate (NCC) with a mean particle diameter of 80 nm and a density of 2.65 g/cm³ was purchased from Shiraishi (Austria) and treated with stearic acid.

2.2 Nano particle surface treatment

Surface treatment of nano calcium carbonate with stearic acid involves coating the particles with a layer of stearic acid. This process is commonly used to improve the dispersion of nano calcium carbonate in polymer matrices, as well as to enhance its compatibility with various polymer systems. The surface treatment is typically carried out using a solution of stearic acid in a solvent like ethanol or toluene. The nano calcium carbonate particles are then added to the solution and stirred or sonicated to ensure uniform coating of the particles with stearic acid. The solvent is then evaporated, leaving behind a thin layer of stearic acid on the surface of the nano calcium carbonate particles. The stearic acid coating can improve the

dispersion of the nano calcium carbonate in polymer matrices by reducing the agglomeration of the particles and promoting better interaction between the filler and the polymer. This can lead to improvements in mechanical properties, thermal stability, and other performance characteristics of the composite materials.

2.3 Samples preparation

To prepare materials for compounding, they were dried in a vacuum oven at 70°C for 16 h. The compounding process was performed using an internal mixer (Brabender Plasticorder W50) with a capacity of 60 cm³. The components were mixed simultaneously in a single step at 170°C and 50 rpm for 10 min (However, to prepare nanocomposites, NCC was added after both polymer components were poured in the brabender). The resulting mixture was then compression molded at 190°C to form sheets of 2 and 3 mm thickness for subsequent measurements.

For the sample preparation, three steps were taken:

Simple blends of PLA/PCL with 15, 25, and 35 wt.% of PCL were prepared to study their mechanical and thermal properties. The blend with 25 wt.% of PCL (P75) showed the best mechanical properties and was selected for further investigations.

Compatibilized PLA/PCL (75/25) blends with varying amounts of GMA compatibilizer (1, 2, 3, and 4 phr) were prepared and their properties were studied.

PLA/PCL nanocomposites with different amounts of NCC (5, 7, 9, and 11 phr) were made and their properties were investigated as well. (The reason why these composition were chosen for NCC was the previous studied that had shown the proportion of NCC in which filler aggregation happened was higher than 15wt.%). We started making sample from 3 phr which was about 2 wt.% and TEM images showed no aggregate. Then we increased amount of NCC to 11 phr (9.7 wt.%) and there was no aggregated particle). So, the aggregate formation can be negligible, even in sample containing 11 phr of NCC).

The Table 1 provides a summary of the names and compositions of the neat polymers, blends, and nanocomposites. For instance, P75G2 represents a nanocomposite sample containing 75 wt.% of PLA, 25 wt.% of PCL, and 2 phr of GMA.

2.4 Characterization

2.4.1 Mechanical characterization

Tensile tests were conducted using a SUN 2500, Galdabini universal testing machine according to ASTM D638 with a strain rate of 5 mm/min at ambient temperature. Five dumbbell-shaped specimens with a thickness of 3 mm were tested for each sample, and the mean values were reported.

Notched Izod impact tests were performed using the Izod Impact Tester (Ueshima Seisakusho, Tokyo, Japan) in accordance with ASTM D256. Three specimens in dimensions of 64 × 12.7 × 6.4 mm were prepared and tested for each sample.

2.4.2 Differential scanning calorimetry (DSC)

Nonisothermal crystallization behavior of the samples was determined using a DSC1, Mettler Toledo differential scanning

TABLE 1 Summarized name and composition of prepared samples.

Samples	PLA (wt.%)	PCL (wt.%)	NCC (phr)	GMA (phr)
P100	100	0	0	0
C100	0	100	0	0
P85	85	15	0	0
P75	75	25	0	0
P65	65	35	0	0
P75G1	75	25	0	1
P75G2	75	25	0	2
P75G3	75	25	0	3
P75G4	75	25	0	4
P75N5	75	25	5	0
P75N7	75	25	7	0
P75N9	75	25	9	0
P75N11	75	25	11	0

calorimeter. The samples were heated from room temperature to 200°C at a rate of 10°C/min and held at this temperature for 5 min to eliminate thermal history. Subsequently, the samples were cooled to room temperature at the same rate and then heated to 200°C at a rate of 10°C/min again.

The crystallinity of the samples was calculated using the cooling process, and melting behavior was assessed through the second heating process. The crystallinity (X_c) was calculated according to Eq. 1.

$$X_c(\%) = \left(\frac{\Delta H_m - \Delta H_{cc}}{\Delta H_m^0 \left(\frac{\phi_{PEL}}{100} \right)} \right) \times 100 \quad (1)$$

In this equation, ΔH_m and ΔH_{cc} refer to the melting and cold crystallization enthalpy of the samples respectively, determined from the DSC thermogram. ϕ_{PLA} represents the weight percentage of PLA in the blends, and ϕ_{PEL} presents the enthalpy of 100% crystalline PLA (93.6 J/g) (Najafi et al., 2012).

2.4.3 Morphology

The morphology of the blends was examined using a scanning electron microscope (SEM) (DSM 960 A, Germany) operated at 10 kV accelerating voltage. The samples were cryogenically fractured after being stored in liquid nitrogen for 15 min. The fracture surface of the samples was coated with gold using a sputter coater to enhance conductivity.

2.4.4 Spectroscopy

Fourier transform infrared analysis (FT-IR) of PLA, PCL, and the prepared samples was conducted over a range of (400–4,000) cm^{-1} with 64 scanning numbers using Spectrum Bomem MB102 and the Attenuated Total Reflectance (ATR) method.

The sample for nuclear magnetic resonance (NMR) analysis was first dissolved in CDCl_3 and sealed in an NMR tube with a 10 mm O.D. Subsequently, after degassing, the analysis was conducted using a Bruker AMX400 ^1H NMR and ^{13}C NMR spectrometers with conditions of 100 MHz, 30 pulse, and 4 s cycle time.

2.4.5 Dynamic mechanical analysis (DMA)

DMA was performed on the samples using (a MK11, Polymer Laboratory). The frequency of testing was set at a fixed rate of 1 Hz, while the dynamic strain applied was 0.025%. The temperature range for the analysis spanned from 60 to 180°C, and the scanning rate was precisely controlled at 2°C per minute.

2.4.6 Molecular weight measurements

Gel Permeation Chromatography (GPC) was carried out using a Waters 2414 refractive index detector, equipped with a Styragel HR5E 7.8 × 300 mm column with a molecular weight resolving range of 2,000–4,000,000. The melt-blended samples were dissolved in distilled tetrahydrofuran (THF) at a concentration of 3.33 mg/mL, and THF was eluted at a rate of 1.0 mL/min at 40°C and calibrated with polystyrene standards.

2.4.7 Rheology

A rheo mechanical spectroscopy (RMS) apparatus, specifically the Anton-Paar 302 model, with parallel plates set at 1 mm distance with a diameter of 25 mm operating at 180°C, was used to study the small amplitude oscillatory shear rheology (SAOS) of the unblended individual polymers, including neat samples, blends with and without compatibilizer, and nanocomposite blends.

TABLE 2 Mechanical properties of neat PLA and PCL and their blends and nanocomposites.

Samples	Tensile modulus (MPa)	Tensile strength (MPa)	Elongation at break (%)	Impact strength (J/m)
P100	2,134 ± 84	59.5 ± 2.4	7.5 ± 0.9	21.6 ± 1.6
C100	286 ± 12	21.2 ± 1.4	>560	-
P85	1873 ± 78	47.6 ± 1.6	16.2 ± 1.2	38.2 ± 1.9
P75	1796 ± 73	43.5 ± 1.3	35.1 ± 1.5	46.1 ± 2.1
P65	1,425 ± 65	38.2 ± 1	26.8 ± 1.4	43.2 ± 1.9
P75G1	1780 ± 71	45.3 ± 0.9	76 ± 3.9	52.6 ± 2.4
P75G2	1722 ± 68	44.8 ± 0.6	92.3 ± 6.1	59.3 ± 2.6
P75G3	1,646 ± 64	42.1 ± 1.2	130.5 ± 8.9	66.3 ± 2.6
P75G4	1,602 ± 64	41.7 ± 1.2	106.9 ± 6.3	61.4 ± 2.2
P75N5	2,589 ± 92	38.4 ± 1.2	4.4 ± 0.7	41.8 ± 2.4
P75N7	2,806 ± 103	35.9 ± 1.8	3.8 ± 0.5	42.3 ± 2.7
P75N9	3,222 ± 149	35.2 ± 0.9	3.1 ± 0.6	43.4 ± 2.9
P75N11	3,409 ± 171	32.8 ± 1.1	2.4 ± 0.1	40.6 ± 2.5

3 Results and discussion

3.1 Mechanical properties

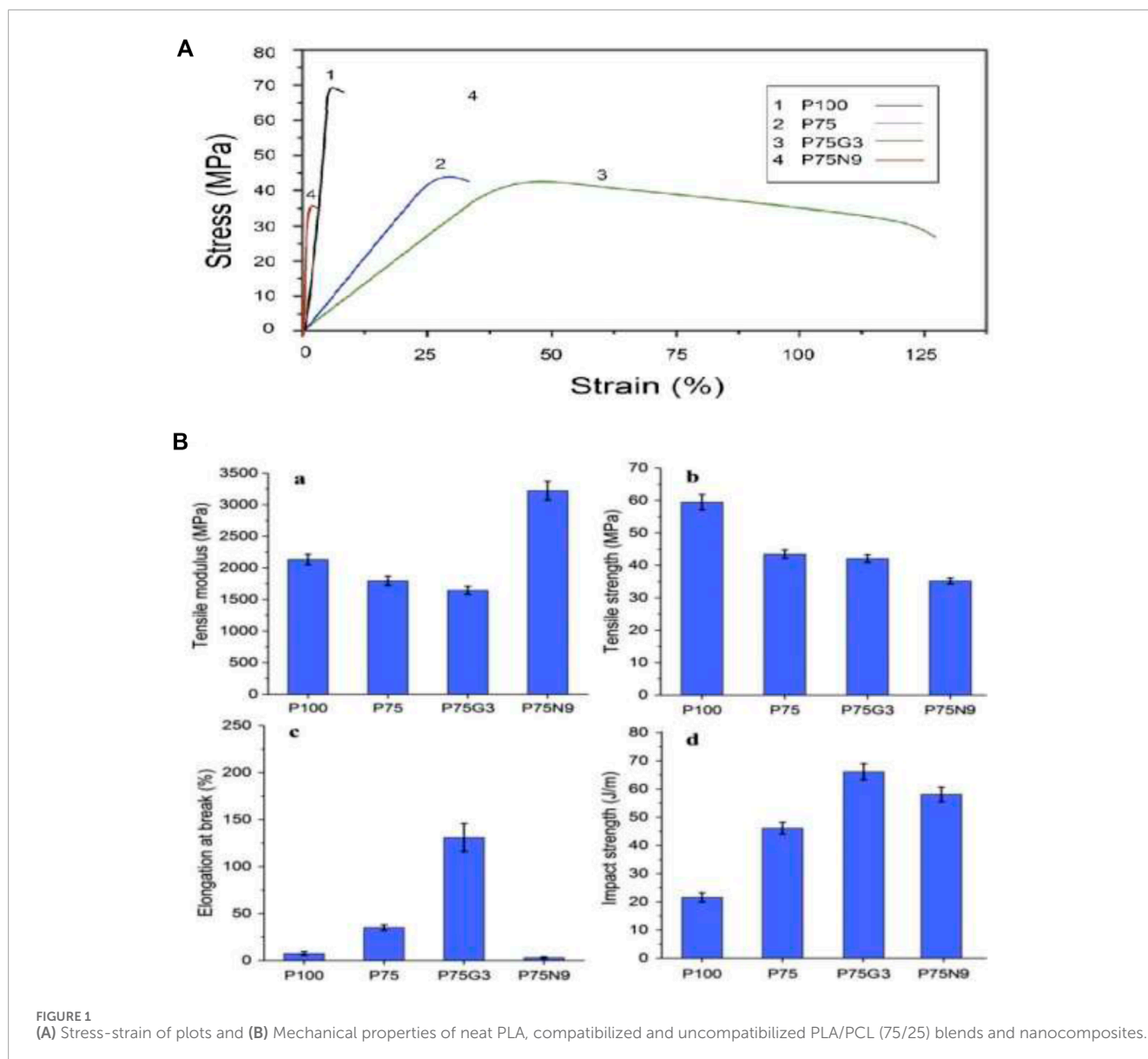
Tensile properties and impact strengths are presented in Table 2 and reveal that incorporating ductile PCL into PLA improved its toughness. For example, 15 wt.% PCL increased the impact strength of neat PLA from 21.6 to 38.2 J/m (P85). Brittle fracture observed in neat PLA indicated a lack of yield phenomenon (Bhatia et al., 2007). However, the presence of PCL introduced a shear yielding mechanism that enhanced the toughness of PLA. Interestingly, the sample containing 25 wt.% of PCL exhibited the highest impact strength and elongation at break among the blends. This maximum is likely attributed to phase separation between PLA and PCL at higher PCL loadings, resulting in poor interfacial adhesion and a decrease in mechanical properties in the blend containing 35 wt.% of PCL (P65), as supported by previous studies (Yeh et al., 2009; Broz et al., 2003). The PLA/PCL blend demonstrates a lower critical solution temperature (LCST), in which the optimum PCL composition for the initiation of phase separation was estimated to be around 36% by volume. Consequently, the PLA/PCL blend with a ratio of 75/25 was selected for further experimentation.

To improve compatibility of PLA and PCL, GMA was employed as a reactive compatibilizer in the blend. Notably, the addition of 1 phr of GMA to P75 increased the elongation at break from 35.1% to 76%. This improvement can be attributed to enhanced compatibility between PLA and PCL, as well as the uniform distribution of PCL droplets facilitated by GMA because of the reduction of interfacial tension (Guerrica-Echevarría et al., 2000; Ayirala and Rao, 2006).

The positive impact of GMA on the mechanical properties of polymer blends has been reported previously (Chee et al., 2013; Juntuek et al., 2012; Kumar et al., 2010). The results presented in Table 2 reveal that increasing content of GMA up to 3 phr further improves the elongation at break and impact strength of the samples. However, exceeding the optimum amount of compatibilizer (3 phr) had an adverse effect on the mechanical properties, potentially due to phase separation. This behavior signifies that an extra quantity of compatibilizer within the blend did not undergo any reaction; therefore, its influence on softening of polymer phases decreased the mechanical properties. In the regions where this unreacted compatibilizer existed, the movement of polymer chains accelerated, as the induced free volume within the system increased. Moreover, a significant rise in elongation at break of polymer blends is attributed to the lubricating effect of GMA, and thus improved fluidity of molecular chain (Aliotta et al., 2020).

In a previous paper, incorporating more than 3 wt.% of GMA into PLA/PCL blends resulted in a decrease in flexural modulus, elongation at break, and impact strength (Chee et al., 2013). Also, Zhang et al. (2009) found that increasing the T-GMA content initially improved the elongation at break, but subsequent increases ultimately reduced this property.

In addition to investigating the effect of NCC on PLA/PCL blends, the impact of different amounts of NCC on uncompatibilized PLA/PCL (75/25) blend was examined. A decrease in tensile strength and elongation at break was seen as the quantity of NCC increased; however, the tensile modulus and impact strength of the samples were increased. The decline in tensile properties can be attributed to reduced chain mobility and the formation of voids during the tensile test, which arose from the discontinuity



in load transfer across the chains. Despite this, the presence of NCC led to an increase in the impact strength of the P75 sample, potentially due to crack growth prevention. Notably, the use of 9 phr NCC yielded the most preferable mechanical properties, as the higher concentration of NCC increased rigidity. Liang et al. (2015) also observed that the tensile yield strength and un-notched Izod impact strength of PLA/PCL/NCC nanocomposite experienced minimal changes as the weight fraction of filler particles exceeded 3 wt.%. Figure 1A depicts the stress-strain plots of tensile test and Figure 1B shows four bar charts including mechanical properties of the selected superior samples from each group. As can be seen in Figure 1A, PCL does not change the brittleness of PLA because of their incompatibility. However, GMA swaps the fracture mode of PLA/PCL from brittle to ductile due to stress transfer along the interface. However, the addition of NCC in uncompatibilized blend results in a more brittle behavior compared to neat PLA.

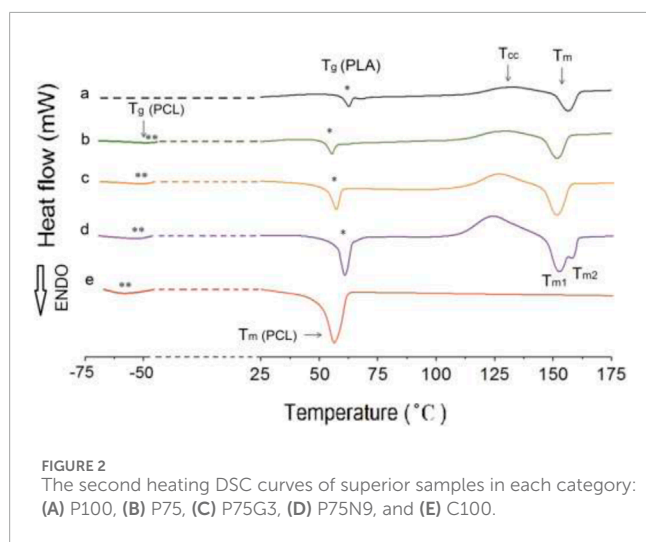
3.2 Thermal properties

The glass transition temperature (T_g) can be used to assess compatibility of polymer blend components. A single T_g indicates a blend that is a single phase. Additionally, variations in cold crystallization temperature (T_{cc}), melting temperature (T_m), and percentage of crystallinity (X_c) are often indicative of the interactions between different components (Li and Huneault, 2011). The obtained DSC results are summarized in Table 3 and selected thermographs are shown in Figure 2. To ensure accurate assessments, the thermal data was analyzed based on the second heating run, which eliminates any potential influence of process history.

The neat PLA demonstrates an orthorhombic structure with a crystallization peak at $T_c = 132^\circ\text{C}$ and a melting peak at $T_m = 157.6^\circ\text{C}$. On the other hand, neat PCL only exhibits a melting peak at $T_m = 55.2^\circ\text{C}$. P75 blend exhibits lower degree of incompatibility

TABLE 3 Thermal properties of neat PLA and PCL and their blends and nanocomposites on the second heating run.

Samples	T_g (°C)	T_{cc} (°C)	T_m (°C)	ΔH_{cc} (J/g)	ΔH_m (J/g)	X_c (%)
P100	62.4	132	157.6	15.01	16.22	1.3
C100	-58.3	-	55.2	-	-	-
P85	54.3	130.9	154.1	15.99	16.85	1.48
P75	57.1	129.2	153.4	16.49	17.54	1.72
P65	56	129.7	153.8	16.83	17.77	1.39
P75G1	57.4	128.6	152.9	16.86	18.21	1.94
P75G2	57.9	128.2	152.6	16.95	18.42	2.12
P75G3	58.3	127.5	152.1	17.19	18.8	2.34
P75G4	58.3	127.9	152.8	17.15	18.68	2.23
P75N5	58.4	127.2	155.6	19.15	22.14	4.31
P75N7	59.6	126.6	157.2	19.57	22.96	4.89
P75N9	60.9	125.8	152.6	19.84	23.74	5.65
			158.9			
P75N11	61.3	126.3	153.1	19.59	23.32	5.43
			160.2			



between PLA and PCL among other blend samples. For samples without NCC or GMA, T_{cc} values for all blends are lower than that of neat PLA, with the P75 blend having the lowest value, suggesting the nucleation effect of PCL. Therefore, the P75 sample composition is selected for subsequent samples.

The impact of varying amounts of GMA compatibilizer on the thermal properties of P75 blend was investigated. GMA decreases the T_g and T_m of P75 due to an increase in polymer chain

mobility. This is attributed to the reactive epoxide group present in GMA, which can react with both PLA and PCL, facilitating the creation of covalent bonds that bridge the two polymer phases. Consequently, this covalent bonding strengthens the interfacial adhesion and promotes efficient stress transfer between the polymers, resulting in improved chain mobility (Kong et al., 2023). Additionally, as the T_g of GMA is lower than both PLA and PCL, its incorporation into the blend leads to an overall reduction in the blend's T_g . This decrease in T_g enhances chain mobility, enabling polymer chain rearrangement and reducing chain entanglements.

In addition, the cold crystallization of PLA in the blend was accelerated after addition of GMA as evidenced by a decrease in T_{cc} and an increase in ΔH_m , in agreement with the findings of Sugih et al. (2009). GMA reduces the size and increases the number of PCL domains and the total area of PLA/PCL interface increases. As a result, the greater the number of PCL domains, the more effective it is as a nucleation agent. In addition, the acceptable effect of GMA on thermal properties of blends took place in the sample containing 3 phr of GMA. The limited interaction capacity between the polymer and compatibilizer led to unreacted GMA, resulting in incompatibility in the P75G4 sample (Chee et al., 2013).

Furthermore, the addition of NCC to the P75 increased the T_g and T_m . The T_{cc} of P75 decreased significantly, indicating that NCC enhances the rate of PLA crystallization. This can be attributed to

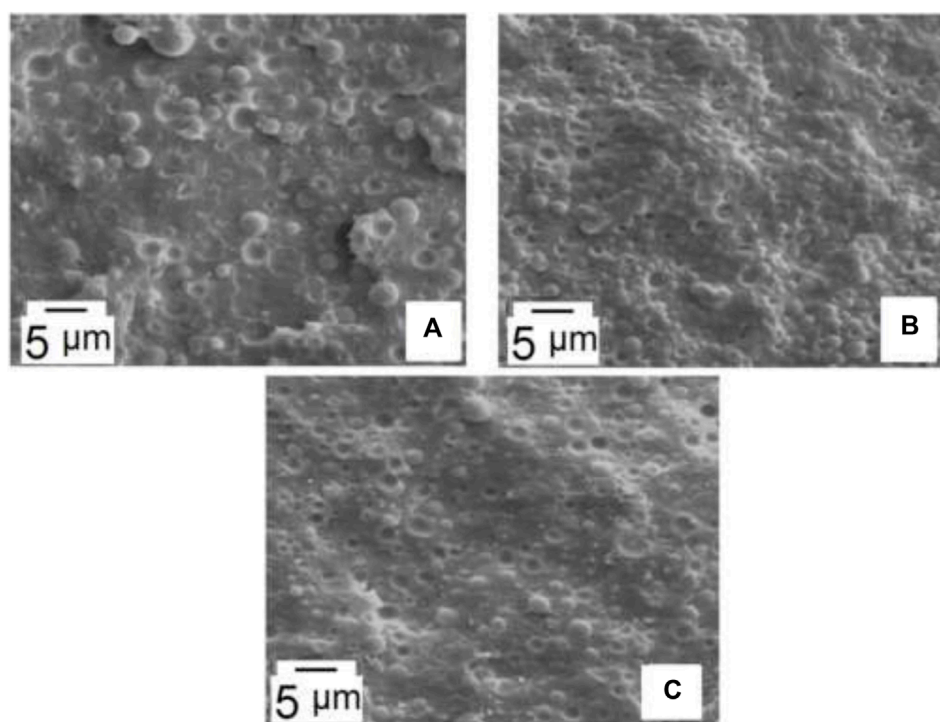


FIGURE 3 SEM micrographs of: (A) P75, (B) P75G3, and (C) P75N9.

the nucleating effect of the nanoparticle. NCC in 9 phr enhanced thermal properties, as evidenced by a distinct increase in the percentage of crystallinity compared to P75 (Balakrishnan et al., 2010; Salehiyan et al., 2015). Besides T_{cc} changes, it was understood that the P75N9 and P75N11 samples exhibit two distinct melting peaks. According to Figure 2D, low temperature melting peak (T_{m1}) should be associated with the fusion of the crystals grown by normal primary crystallization, whereas the high-temperature melting peak (T_{m2}) is related to the melting peak of the most perfect crystals after rearrangement during the second heating process (Tábi et al., 2010; Huang et al., 2009). This phenomenon happened because of the increment in NCC composition, which prompted reduction of chain mobility and prevented the lamellas from being completed. Therefore, some imperfect crystals with lower lamella's thickness are formed; consequently, double peaks for T_m are seen. Moreover, it is found that the use of 11 phr of NCC in the P75N11 did not make favorable changes in T_{cc} and X_c compared to the P75N9. It seems that the nucleating effect of NCC is restricted due to nanoparticle aggregation. It is important to take into consideration that the process of crystallization is divided into two stages: nucleation and growth of lamellas (De Santis et al., 2011). The addition of both NCC and GMA enhances nucleation, but the effectiveness of NCC is superior. However, NCC hinders the growth of lamellas by restricting molecular chain movement and resulting in the formation of imperfect lamellas. On the other hand, GMA increases chain mobility and facilitates the arrangement of chains within the lamellas. So, GMA counteracts the formation of imperfect crystals and alters the characteristics of the samples at their melting point.

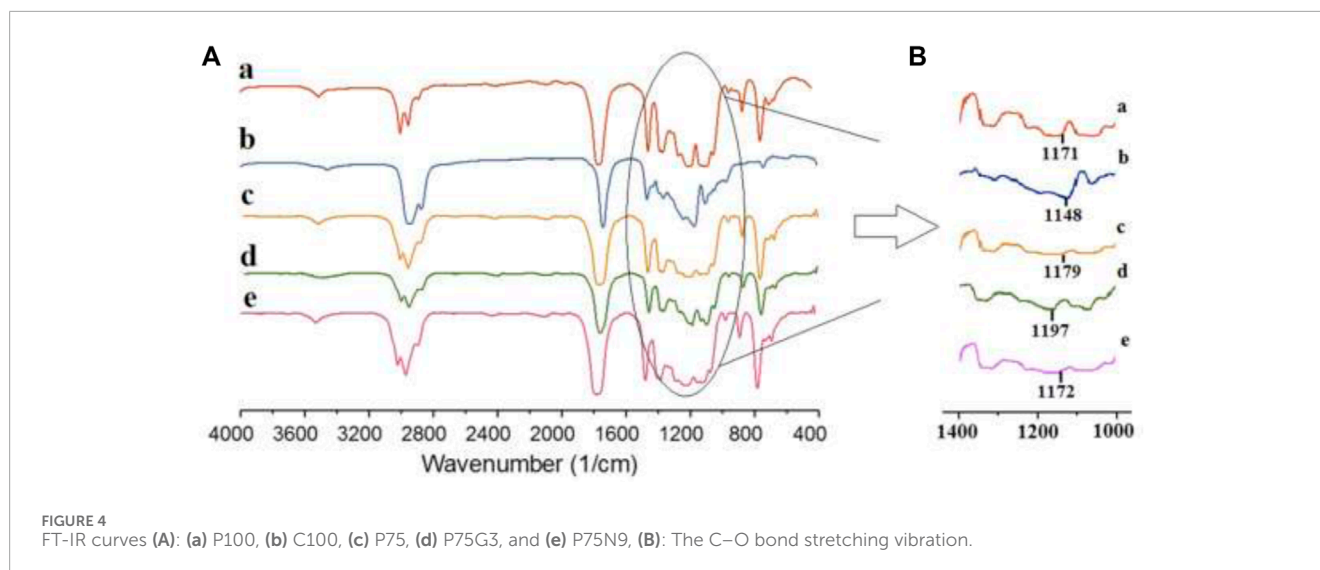
TABLE 4 PCL droplets sizes for PLA/PCL blends and their nanocomposites.

Samples	Range of PCL droplets diameter (μm)	PCL droplets average diameter (μm)
P75	4.8–10.2	7.6
P75G3	2.2–6.4	4.6
P75N9	3.4–7	5.8

(GMA does not have T_g as it is a material with molecular weight of 142 g/mol).

3.3 Morphology

In Figure 3, SEM images of P75, P75G3, and P75N9 samples are displayed. All samples exhibit droplet-matrix morphology. The circular structures in the dispersed phase represent the PCL domains. Table 4 presents the results of particle size determined using ImageJ software. In Figure 3A, the micrograph of P75 suggests poor interfacial adhesion between the PLA matrix and PCL domains, indicating complete incompatibility of these two polymers, which is supported by previous studies (Yeh et al., 2009; Broz et al., 2003; Rodriguez et al., 2006). A similar structure is observed in P75G3 (Figure 3B), with smaller PCL droplets compared to those



in P75, showing improved compatibility of polymers. The positive effect of GMA on modifying the interfacial adhesion of PLA/PCL was also reported (Chee et al., 2013). In addition, SEM analysis demonstrated that the incorporation of GMA into PLA/PCL resulted in enhanced compatibility by promoting multiple crazing and cavitation mechanisms. The same conclusion according to SEM analysis was made as an evidence of improved compatibility between maleated SEBS and PLA/cellulose nanocrystal (Diani et al., 2016).

In the case of the P75N9 sample (Figure 3C), the size of PCL domains is smaller compared to P75, but larger than those in P75G3. These results suggest that NCC can also act as a compatibilizer for the PLA/PCL. This incident may be due to the steric hindrance of nanoparticles in the merging of PCL droplets.

3.4 Spectroscopy

3.4.1 Fourier transform infrared analysis (FT-IR)

FT-IR was carried out and spectra of the samples are shown in Figure 4A. The peaks in the range of 3,400–3,600 cm^{-1} correspond to O–H group stretching vibrations, while the peaks around 2,800–3,000 cm^{-1} are associated with the symmetric stretching vibration of CH groups in saturated hydrocarbons. The intense peak at around 1760 cm^{-1} is attributed to C=O stretching vibrations. Several weaker peaks in the range of 1,050–1,250 cm^{-1} are assigned to C–O from carboxyl groups and C–O–C stretching vibrations. Three peaks at 1,300–1,500 cm^{-1} may be attributed to the vibration of C–H in CH_3 groups.

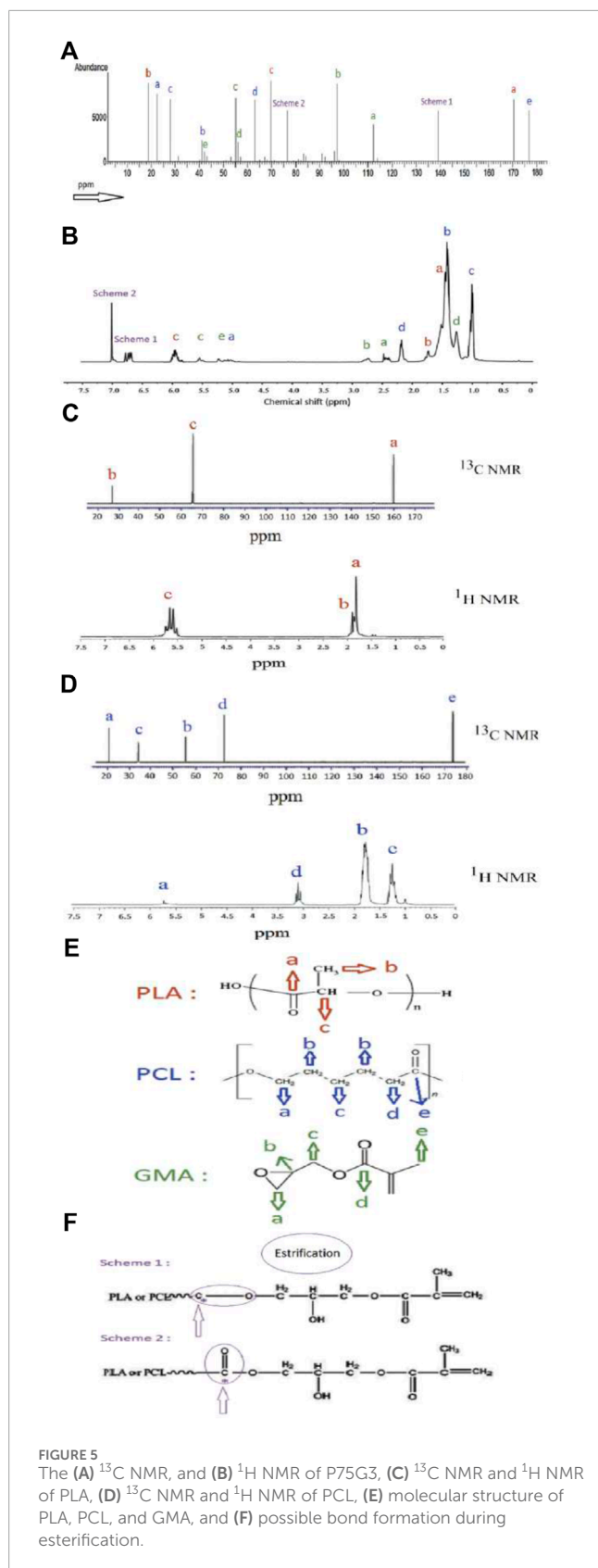
The absence of significant shifts in wavenumbers between P75 and P100 suggests no interactions between PLA and PCL upon blending. In P75G3, the C=O stretching vibration remained nearly unchanged, indicating no reaction on the C=O bonds of PLA and PCL backbone chains. Figure 4B illustrates the C–O bond stretching vibration, indicating a noticeable shift when GMA is introduced into blend. This suggests reactions between the hydroxyl groups of PLA and PCL with the epoxy group of GMA, potentially increased compatibility. Furthermore, the FT-IR peaks of P75N9 and P75 exhibit subtle changes. In addition to the steric hindrance effect

caused by NCC, it is deduced that the presence of stearic acid on the surface of NCC slightly absorbed polymer chains. This observation corresponds with previous works suggesting that steric hindrance plays a role in morphology stabilization in nanocomposites in the presence of nanoparticles (Vermant et al., 2004; Vignati et al., 2003). It is also highlighted that the localization of nanoparticles at the polymer interface leads to higher compatibility between the two polymers.

3.4.2 Nuclear magnetic resonance (NMR)

NMR is a highly efficient technique for determining the composition of unknown materials and accurately identifying reactions between different materials during the mixing process. In this study, NMR was performed solely on the PLA, PCL, and compatibilized blend, as there were no expected reactions during the mixing of PLA/PCL with nano calcium carbonate. As depicted in Figure 5, the reactions between the hydroxyl and carboxyl groups of PLA and PCL with the epoxy group of GMA were observed in two separate schemes, 1 and 2, with peaks at 76.3 and 139.1 ppm in ^{13}C NMR, and 6.7 and 7.1 ppm in ^1H NMR. These peaks are believed to originate from a methylene unit ($-\text{O}-\text{CH}_2-\text{CH}_3$) produced during the melt-blending process, primarily through chain extension due to potentially involving esterification. GMA also caused noticeable changes in peaks related to the carbon functional groups of both polymers, bringing them closer together compared to their original state, as observed in previous study (Tuancharoensri et al., 2023). The longer chains of PLA and PCL played a beneficial compatibilizing role by providing only one possible reaction site. In contrast, chain extender agents such as Joncryl ADR with a higher number of reaction sites can sometimes lead to phase separation due to uncontrolled cross-linking reactions, while chain scission can also deteriorate chain extension process and cause a decrease in properties.

In ^1H NMR, PLA exhibits peaks at 5.13 and 1.56 ppm, corresponding to protons in the methylene unit and methyl unit, respectively. PCL shows peaks at 4.07, 2.29, and 1.38 ppm, representing protons in methylene units at different positions on the backbone. GMA displays peaks at 2.33, 1.64, and 0.93 ppm,



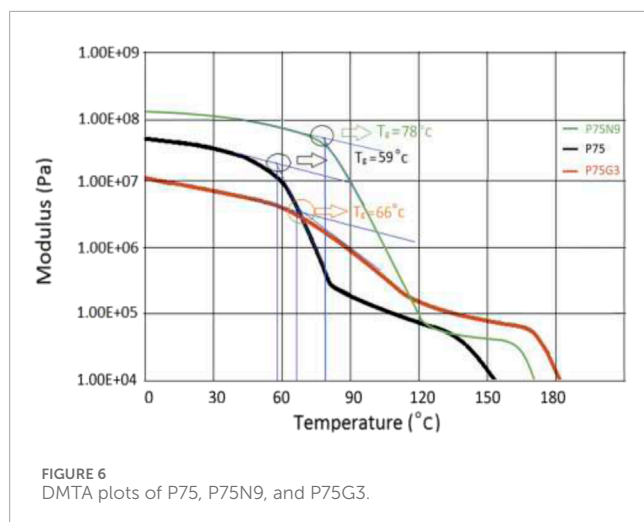
representing methylene, methylene, along with a peak at 2.11 ppm for the methyl unit in the carboxyl side group and peaks at 3.29–5.47 ppm for the hydroxyl backbone.

In ^{13}C NMR, PLA exhibits peaks at 16.7, 69.1, and 177.3 ppm for methyl, methylene, and carbonyl carbons, respectively. PCL displays peaks at 24.7–25.6, 28.5, 34.2, and 64.2 ppm for four methylene carbons and a peak at 173.8 ppm for the carbonyl carbon. GMA shows peaks at 100.2, 73.0, 72.5, 76.8, and 71.9 ppm for the backbone, 62.3 ppm for the methylene carbon, 170.1 and 35.9 ppm for the carbonyl and methyl carbons in the acetate side group, and 172.6, 21.0, 18.7, and 13.8 ppm for the carbonyl carbon, methylene carbons, and methyl carbon in the epoxy side group. Hu et al. (Ye et al., 2023) in another study reported that in PLA/PCL/PLA-g-GMA blend, besides the PLA peaks, PLA-g-GMA exhibited ^{13}C signal peaks at 49.74 and 44.98 ppm, as well as ^1H signal peaks at 3.25 and 2.85 ppm. These peaks corresponded to the chemical shift of epoxy groups, suggesting successful grafting of GMA onto the PLA structure.

3.5 Dynamic mechanical analysis (DMA)

The main goal of the DMA is to study T_g and investigate the molecular interactions within the amorphous and crystalline regions of polymers (Hou and Qu, 2019). As can be seen in Figure 6, nanoparticles in P75N9 led to a higher modulus compared to P75G3. However, the modulus of P75N9 experienced a quicker decrease as the temperature increases. This can be attributed to the rearrangement of NCC particles and transformation of nanoparticle network. The introduction of nanoparticles served to restrict the mobility of polymer chains, thus impeding their movement. Consequently, this resulted in a decline in molecular motions, which in turn contributed to a rise in the overall modulus of the nanocomposite. As the temperature increased, the role of nanoparticles as physical barriers became less prevalent, hindering the deformability and movement of polymer chains. Thus, this led to a significant decrease in modulus. Generally, nanoparticles often possess a considerable surface area and can form robust interactions with polymer chains. These interactions facilitate load transfer between the nanoparticles and the matrices, boosting their bond formation. However, due to the increased temperature, polymer internal chain segments tend to detach from the surface of nanoparticles due to higher relative motional freedom (Tham et al., 2022). Moreover, because of conformational changes at higher temperatures, well-dispersed nanoparticles become less abundant within the polymer matrix, giving rise to formation of defects and regions of lower stiffness. Differences between steric (entropic) states with nanoparticle, does not allow polymer chains to replenish nanoparticles previous position completely. These localized regions characterized by reduced modulus contribute to an overall decline in modulus during DMA. Lastly, as the temperature increases, nanoparticles tend to aggregate or cluster, particularly if they possess a strong mutual attraction, such as NCC particles. These clusters of nanoparticles are susceptible for stress concentration, leading to a drop in the overall modulus (Banerjee and Ray, 2021).

In contrast, the glass transition region of P75G3 appeared in mild slope due to the increased compatibility and notable interaction between PLA and PCL compared to the P75N9. Additionally, the P75G3 exhibited a higher modulus and length in the rubbery region, which can be attributed to the effective performance of GMA in increasing chain extension, enhancing intermolecular



entanglements, and promoting mutual attractions among the ends of PLA and PCL chains. (These are solid evidence to prove the formation of longer chains in P75G3).

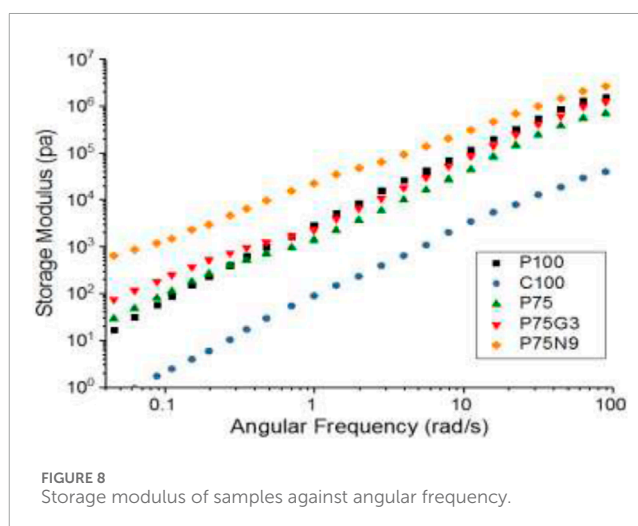
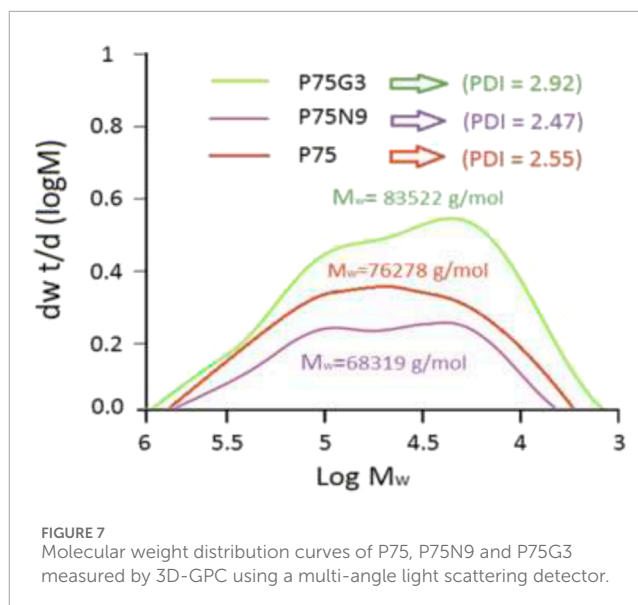
3.6 Gel Permeation Chromatography (GPC)

The molecular weight distribution was determined using GPC with the Mark-Houwink-Sakurada parameters provided by Huang et al. (2003). The average molecular weight of polylactic acid is approximately 218,000 g/mol, while the average molecular weight of polycaprolactone is around 75,000 g/mol. In addition, weight-average molecular weight (M_w) and polydispersity index (PDI) were measured for P75, P75N9 and P75G3 (Figure 7). The results showed the desirable effect of GMA on molecular weight and distribution of P75. Surprisingly, M_w of P75N9 was significantly lower than that of the P75G3. Previous studies have also shown that the presence of GMA as a chain extender can increase the average molecular weight of the polymer formed (Pasanphan et al., 2021; Javadzadeh et al., 2020). The difference in average molecular weight between P75N9 (68,319 g/mol) and P75G3 (83,522 g/mol), and greater PDI value in P75G3, are attributed to the presence of longer and shorter polymer chains. The introduction of GMA led to longer and lower molecular weight chains, as well as a wider distribution. However, the presence of nanoparticles resulted in shorter chains with a narrower distribution.

GMA led to intermingling of adjacent chains, resulting in a higher molecular weight for P75G3 compared to P75N9. This also made molecular weight distribution wider. However, NCC nanoparticles might interfere with the chain extension process, potentially resulting in their scission during mixing (Castilla-Cortázar et al., 2019). This could be due to collision of the nanoparticles and chains.

3.7 Rheological properties

Small amplitude oscillatory shear (SAOS) test were conducted to study the rheology of samples, with the aim of understanding the



relationship between their molecular structures and flow properties. The plots of storage modulus (G') and complex viscosity (η^*) as a function of angular frequency are presented in Figures 8, 9, respectively.

Figure 8 demonstrates that both neat PLA and PCL exhibit a terminal behavior, where the storage modulus G' is proportional to the angular frequency ω^2 . Additionally, the storage modulus of PCL is significantly lower than that of PLA across all frequencies. When PCL is added to PLA, the storage modulus increases at low frequencies, while the storage modulus of P75 is lower than that of pure PLA at medium and high frequencies, indicating a weak interfacial interaction between polymers. However, GMA leads to higher storage modulus compared to uncompatibilized blend. Nevertheless, beyond 1 rad/s, the storage modulus of P75G3 becomes smaller than that of PLA, suggesting partially enhancement the interfacial adhesion between the polymers. Storage modulus of the nanocomposite (P75N9) is notably higher than that of the other samples, aligning with the findings of previous research on polymer blends

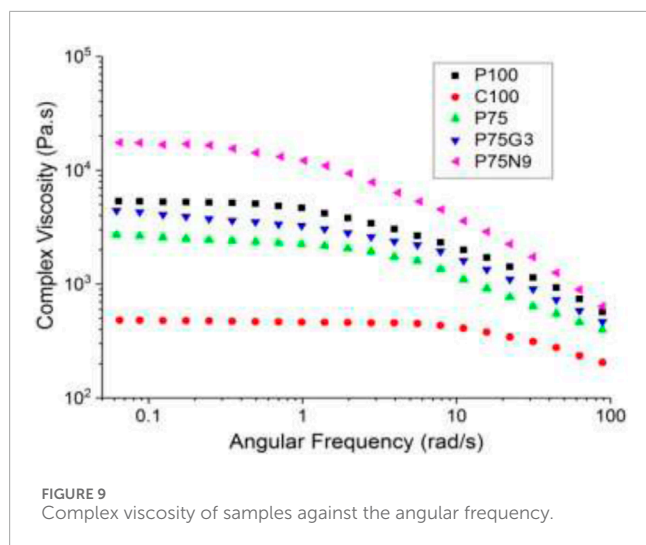


FIGURE 9 Complex viscosity of samples against the angular frequency.

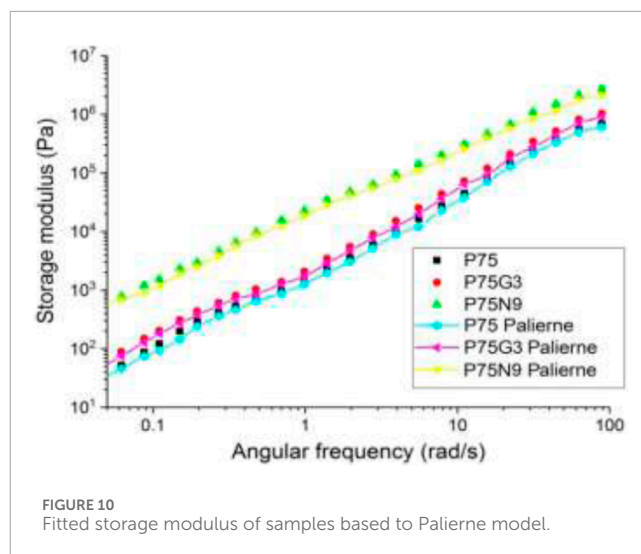


FIGURE 10 Fitted storage modulus of samples based to Palierne model.

TABLE 5 Slope of G' versus ω plots (N), in the range of 0.01–0.1 rad/s and absolute value of degree of shear-thinning (n) for selected samples.

Samples	N	n
P100	1.76	0.39
C100	1.83	0.27
P75	1.44	0.34
P75G3	1.38	0.36
P75N9	0.87	0.62

incorporating nanoparticles (Najafi et al., 2012; Zachariah et al., 2014). Moreover, the appearance of G' plateau at low frequencies in the nanocomposite sample indicates the formation of a three-dimensional network of nanoparticles, resulting in a solid-like behavior. The slope of G' versus ω plots, denoted as (N), was investigated in the range of 0.01–0.1 rad/s and is shown in Table 5. The results reveal that the blend has a lower initial slope of G' than PLA, showing the formation of entangled structures in PLA/PCL melts. GMA has a minimal effect on this slope, as the low molecular weight compatibilizer has a negligible impact on increasing the entanglement density. Furthermore, the outset slope of the G' versus ω plot in P75N9 is much lower than that of neat polymers and compatibilized blends, suggesting nanoparticle aggregation (DEFENG WU et al., 2007; Huitric et al., 2009).

Additionally, the storage modulus plots of the blends exhibit a secondary plateau attributed to the shape relaxation of the PCL dispersed phase PCL (Elias et al., 2007). GMA widens this plateau, because of improved compatibility between PLA and PCL. The frequency dependence of complex viscosity for all samples is depicted in Figure 9. It is evident GMA influences the rheological behavior of P75, leading to an increase in complex viscosity due to enhanced connectivity between the PLA and PCL chains. Similarly, the incorporation of NCC particles into PLA/PCL blends significantly alters their rheological properties, resulting in a notable increase in complex viscosity, especially at low frequencies. Some

researchers corresponded the observation of this plateau to the location of nanoparticles at the interface between two polymer phases (Vinckier et al., 1999a; Vinckier et al., 1999b). The outcomes of previous study demonstrated that a huge increase in the quantity of NCC particles present within the interface triggered the formation of aggregates along the polymer interface (Liu et al., 2024). This consequently impeded a consistent shape relaxation within the polymer interface owing to the substantial difference in the degree of molecular mobility between the polymer chains in the bulk and the interface. Subsequently, this phenomenon leads to the formation of a distinct separated phase in the proximity of the interface.

Additionally, it is obvious that interactions between nanoparticle and polymer, as well as particle-particle interactions, making a substantial increase in the complex viscosity of nanocomposite sample, particularly at low frequencies. High frequency measurements revealed that all samples exhibited pseudoplastic behavior, but neat PCL only displayed Newtonian behavior within a limited frequency range (up to 10 rad/s), on the other hand, P75N9 has a smaller frequency range for Newtonian behavior. The viscosity reduction after the Newtonian region, as determined by the degree of shear-thinning (n), known as power-law index, was more pronounced in the nanocomposite sample compared to other samples (Wagener and Reisinger, 2003).

$$\eta = A\omega^n \tag{2}$$

The value of n was calculated using Eq. 2 in its logarithmic form, and the results are presented in Table 5. It was observed that the P75N9 exhibit more intense shear-thinning behavior compared to the other samples. At higher frequencies, this shear-thinning behavior becomes more evident due to the dispersion of nanoparticle clusters along the direction of shear.

Rheological study of the samples was developed using the Palierne model. This model provides valuable information on the interfacial properties of incompatible PLA/PCL blend and nanocomposite (Lacroix and Carreau, 1997). In the Palierne model, complex modulus of matrices and polymer interface have been utilized to predict the complex modulus of samples (Genoyer, 2018). The aim of this study is to elucidate the relaxation mechanisms

based on polymer chain movements, droplet shape evolution, and relaxation caused by Marangoni stresses (Jacobs et al., 1999). The plots obtained from SAOS test were compared with the plots generated by the Palierne model to assess their overlap. This model is expressed as Eqs 3, 4:

$$G^*(\omega) = G_m^*(\omega) \frac{1 + 3\phi H(\omega)}{1 - 2\phi H(\omega)} \quad (3)$$

$$H(\omega) = \frac{4\left(\frac{\alpha}{R}\right)[2G_m^*(\omega) + 5G_d^*(\omega)] + [G_d^*(\omega) - G_m^*(\omega)][16G_m^*(\omega) + G_d^*(\omega)]}{40\left(\frac{\alpha}{R}\right)[G_m^*(\omega) + G_d^*(\omega)] + [2G_d^*(\omega) + 3G_m^*(\omega)][16G_m^*(\omega) + G_d^*(\omega)]} \quad (4)$$

where α represents the interfacial tension, ϕ represents the volume fraction of dispersed phase, R represents the dispersed particle radius, and represent the complex modulus of the dispersed phase and matrix, respectively.

The simplified Palierne model with the approximation of Graebling et al. (Graebling et al., 1993) was used, where the surface dilatation modulus and surface shear modulus were ignored. The fitting program was assigned an initial value of 100 for α/R , and the optimum value was found to be 76.31 N/m². Using Table 4, the interfacial tension was calculated to be 0.29 mN/m for PCL droplets with an average diameter of 7.6 μ m for P75. Also, P75N9 and P75G3 were compared with R_v extracted from Table 4 and the same interfacial tension (Fenni et al., 2020).

As shown in Figure 10, the Palierne predictions for P75N9 and P75G3 showed a discrepancy in the actual value. It is assumed that in the P75N9, the NCC particles are located both at the interface and in polymer phases, which does not mean that particles saturated the interface, but rather that excessive amounts of NCC were located in the droplets, hindering their shape relaxation (Liao et al., 2020). In the case of sample P75G3, there was more similarity between the fitted plot and the experimental one. Therefore, the effect of GMA on the compatibility of polymers is more remarkable, partially increased their interfacial adhesion during the mixing procedure.

4 Conclusion

In conclusion, the incorporation of GMA and NCC into PLA/PCL blends and nanocomposites had significant impacts on their mechanical, thermal, morphology, and rheological properties. GMA was found to enhance elongation at break and impact strength, while NCC increased tensile modulus and impact strength. DSC analysis revealed changes in PLA crystallinity due to the presence of GMA and NCC, with NMR and FT-IR spectroscopic analyses confirming the reaction between GMA and polymeric chains. GPC plots showed a change in molecular weight distribution with the addition of GMA, leading to longer chains in the polymer. DMA results indicated a higher Tg in nanocomposites and compatibilized

blends compared to neat polymers, while rheological studies demonstrated increased storage modulus and complex viscosity in the presence of GMA and NCC. The Palierne model suggested hindered elastic response at intermediate frequencies due to NCC localization, while the elastic response of the PCL dispersed phase in the compatibilized blend was noticeably different after the addition of GMA. Overall, this study highlights the potential of GMA and NCC in improving the properties of PLA/PCL blends and nanocomposites (Hoffmann et al., 2000; Na et al., 2002; Shi et al., 2011; Eslami and Kamal, 2013; Aid et al., 2017; Rocha et al., 2020; Chow et al., 2022; Xu et al., 2022).

Data availability statement

The original contributions presented in the study are included in the article/supplementary material, further inquiries can be directed to the corresponding author.

Author contributions

MN: Writing–review and editing, Writing–original draft, Visualization, Validation, Software, Resources, Investigation, Funding acquisition, Formal Analysis, Data curation. AJ: Writing–review and editing, Methodology, Conceptualization. HG: Writing–review and editing, Validation, Project administration.

Funding

The author(s) declare that no financial support was received for the research, authorship, and/or publication of this article.

Conflict of interest

The authors declare that the research was conducted in the absence of any commercial or financial relationships that could be construed as a potential conflict of interest.

Publisher's note

All claims expressed in this article are solely those of the authors and do not necessarily represent those of their affiliated organizations, or those of the publisher, the editors and the reviewers. Any product that may be evaluated in this article, or claim that may be made by its manufacturer, is not guaranteed or endorsed by the publisher.

References

Agarwal, S. (2020). Biodegradable polymers: present opportunities and challenges in providing a microplastic-free environment. *Macromol. Chem. Phys.* 221, 1–7. doi:10.1002/macp.202000017

Aid, S., Eddhahak, A., Ortega, Z., Froelich, D., and Tcharkhtchi, A. (2017). Experimental study of the miscibility of ABS/PC polymer blends and investigation of the processing effect. *J. Appl. Polym. Sci.* 134 (25), 44975. doi:10.1002/app.44975

- Aliotta, L., Gigante, V., Acucella, O., Signori, F., and Lazzeri, A. (2020). Thermal, mechanical and micromechanical analysis of PLA/PBAT/POE-g-GMA extruded ternary blends. *Front. Mater.* 7, 1–14. doi:10.3389/fmats.2020.00130
- Al-ityr, R., Lamnawar, K., and Maazouz, A. (2014). Rheological, morphological, and interfacial properties of compatibilized PLA/PBAT blends. *Rheol. Acta* 53, 501–517. doi:10.1007/s00397-014-0774-2
- Arrieta, M. P., Samper, M. D., Aldas, M., and López, J. (2017). On the use of PLA-PHB blends for sustainable food packaging applications. *Mater. (Basel)* 10, 1008–1026. doi:10.3390/ma10091008
- Ayrala, S. C., and Rao, D. N. (2006). Solubility, miscibility and their relation to interfacial tension in ternary liquid systems. *Fluid Phase Equilib.* 249, 82–91. doi:10.1016/j.fluid.2006.09.020
- Balakrishnan, H., Hassan, A., Wahit, M. U., Yussuf, A. A., and Razak, S. B. A. (2010). Novel toughened polylactic acid nanocomposite: mechanical, thermal and morphological properties. *Mater. Des.* 31, 3289–3298. doi:10.1016/j.matdes.2010.02.008
- Banerjee, R., and Ray, S. S. (2021). An overview of the recent advances in polylactide-based sustainable nanocomposites. *Polym. Eng. Sci.* 61, 617–649. doi:10.1002/pen.25623
- Bhatia, A., Gupta, R. K., Bhattacharya, S. N., and Choi, H. J. (2007). Compatibility of biodegradable poly (lactic acid) (PLA) and poly (butylene succinate) (PBS) blends for packaging application. *Korea Aust. Rheol.* 19 (3), 125–131.
- Broz, M. E., Vanderhart, D. L., and Washburn, N. R. (2003). Structure and mechanical properties of poly (d, l -lactic acid)/poly (ε-caprolactone) blends. *Biomaterials* 24, 4181–4190. doi:10.1016/s0142-9612(03)00314-4
- Castilla-Cortázar, I., Vidaurre, A., Marí, B., and Campillo-Fernández, A. J. (2019). Morphology, crystallinity, and molecular weight of poly(ε-caprolactone)/graphene oxide hybrids. *Polym. (Basel)* 11, 1099. doi:10.3390/polym11071099
- Chee, W. K., Ibrahim, N. A., Zainuddin, N., Abd Rahman, M. F., and Chieng, B. W. (2013). Impact toughness and ductility enhancement of biodegradable poly (lactic acid)/poly (caprolactone) blends via addition of glycidyl methacrylate. *Adv. Mater. Sci. Eng.* 2013, 1–8. doi:10.1155/2013/976373
- Chen, Y., Lu, T., Ke, F., Zhang, H., and Wang, H. (2023). Fully biodegradable PLA composite with improved mechanical properties via 3D printing. *Materials Lett.* 331, 133543. doi:10.1016/j.matlet.2022.133543
- Cheng, Y., Han, H., Fang, C., Li, H., Huang, Z., and Su, J. (2020). Preparation and properties of nano-CaCO₃/waste polyethylene/styrene-butadiene-styrene block polymer-modified asphalt. *Polym. Compos.* 41 (2), 614–623. doi:10.1002/pc.25392
- Chow, H. M., Koay, S. C., Choo, H. L., Chan, M. Y., and Ong, T. K. (2022). Investigating effect of compatibilizer on polymer blend filament from post-used styrofoam and polyethylene for fused deposition modelling. *J. Phys. Conf. Ser.* 2222, 012006. doi:10.1088/1742-6596/2222/1/012006
- Chuaponpat, N., Ueda, T., Ishigami, A., Kurose, T., and Ito, H. (2020). Morphology, thermal and mechanical properties of co-continuous porous structure of PLA/PVA blends by phase separation. *Polym. (Basel)* 12 (1083), 1083. doi:10.3390/polym12051083
- Defeng Wu, M. Z., Liang, W. U., Sun, YURONG, and Zhang, M. (2007). Rheological properties and crystallization behavior of multi-walled carbon nanotube/poly(ε-caprolactone) composites. *J. Polym. Sci. Part B Polym. Phys.* 45, 3137–3147. doi:10.1002/polb.21309
- De Santis, F., Pantani, R., and Titomanlio, G. (2011). Nucleation and crystallization kinetics of poly(lactic acid). *Thermochim. Acta* 522, 128–134. doi:10.1016/j.tca.2011.05.034
- Diani, J., Gall, K., and Nayak, S. (2016). Toughening of polylactic acid using styrene ethylene butylene styrene: mechanical, thermal, and morphological studies. *Polym. Eng. Sci.* 56 (6), 669–675. doi:10.1002/pen.24293
- Dorgan, J. R., Williams, J. S., and Lewis, D. N. (1999). Melt rheology of poly(lactic acid): entanglement and chain architecture effects. *J. Rheol. (N. Y. N. Y.)* 43 (5), 1141–1155. doi:10.1122/1.551041
- Elias, L., Fenouillot, F., Majeste, J. C., and Cassagnau, P. (2007). Morphology and rheology of immiscible polymer blends filled with silica nanoparticles. *Polym. Guildf.* 48, 6029–6040. doi:10.1016/j.polymer.2007.07.061
- Eslami, H., and Kamal, M. R. (2013). Effect of a chain extender on the rheological and mechanical properties of biodegradable poly (lactic acid)/poly [(butylene succinate) co -adipate] blends. *Appl. Polym. Sci.* 153, 2418–2428. doi:10.1002/app.38449
- Farah, S., Anderson, D. G., and Langer, R. (2016). Physical and mechanical properties of PLA, and their functions in widespread applications — a comprehensive review. *Adv. Drug Deliv. Rev.* 107, 367–392. doi:10.1016/j.addr.2016.06.012
- Fenni, S. E., Wang, J., Haddaoui, N., Favis, B. D., Müller, A. J., and Cavallo, D. (2020). Nucleation of poly(lactide) partially wet droplets in ternary blends with poly(butylene succinate) and poly(ε-caprolactone). *Macromolecules* 53, 1726–1735. doi:10.1021/acs.macromol.9b02295
- Ferrer, I., Manresa, A., Méndez, J. A., Delgado-Aguilar, M., and Garcia-Romeu, M. L. (2021). Manufacturing PLA/PCL blends by ultrasonic molding technology. *Polym. (Basel)* 13 (2412), 2412. doi:10.3390/polym13152412
- Fortelny, I., Ujčić, A., Fambri, L., and Slouf, M. (2019). Phase structure, compatibility, and toughness of PLA/PCL blends: a review. *Front. Mater.* 6, 1–13. doi:10.3389/fmats.2019.00206
- Gao, H., Li, J., Li, Z., Li, Y., Wang, X., Jiang, J., et al. (2023). Enhancing interfacial interaction of immiscible PCL/PLA blends by *in-situ* crosslinking to improve the foamability. *Polym. Test.* 124, 7–16. doi:10.1016/j.polymertesting.2023.108063
- Genoyer, J. (2018). Compatibilization of PMMA/PS blends by nanoparticles and block copolymers: effect on morphology and interfacial relaxation phenomena. <https://core.ac.uk/download/pdf/162151614.pdf>.
- Graebbling, D., Muller, R., and Palierne, J. F. (1993). Linear viscoelastic behavior of some incompatible polymer blends in the melt. Interpretation of data with a model of emulsion of viscoelastic liquids. *Macromolecules* 26, 320–329. doi:10.1021/ma00054a011
- Guerrica-Echevarría, G., Eguiazábal, J. I., and Nazábal, J. (2000). Interfacial tension as a parameter to characterize the miscibility level of polymer blends. *Polym. Test.* 19 (7), 849–854. doi:10.1016/s0142-9418(99)00055-0
- Guo, R., Ren, Z., Bi, H., Xu, M., and Cai, L. (2019). Electrical and thermal conductivity of polylactic acid (PLA)-based biocomposites by incorporation of nanographite fabricated with fused deposition modeling. *Polym. (Basel)* 11 (549), 29–41. doi:10.3390/polym11030549
- Harada, M., Iida, K., Okamoto, K., Hayashi, H., and Hirano, K. (2008). Reactive compatibilization of biodegradable poly (lactic acid)/poly (caprolactone) blends with reactive processing agents. *Polym. Eng. Sci.* 48, 1359–1368. doi:10.1002/pen.21088
- Hoffmann, B., Kressler, J., Stöppelmann, G., Friedrich, C., and Kim, G.-M. (2000). Rheology of nanocomposites based on layered silicates and polyamide-12. *Colloid Polym. Sci.* 278, 629–636. doi:10.1007/s003960000294
- Hou, A.-L., and Qu, J.-P. (2019). Super-Toughened poly (lactic acid) with poly(ε-caprolactone) and ethylene-methyl acrylate-glycidyl methacrylate by reactive melt blending. *Polym. (Basel)* 11 (771), 771. doi:10.3390/polym11050771
- Huang, J.-W., Hung, Y. C., Wen, Y.-L., Kang, C.-C., and Yeh, M.-Y. (2009). Polylactide/nano- and micro-scale silica composite films. II. Melting behavior and cold crystallization. *Appl. Polym. Sci.* 112, 3149–3156. doi:10.1002/app.29699
- Huang, S., Wang, H., Ahmad, W., Ahmad, A., Vatin, N. I., Mohamed, A. M., et al. (2022). Plastic waste management strategies and their environmental aspects: a scientometric analysis and comprehensive review. *Int. J. Environ. Res. Public Health* 19 (8), 4556. doi:10.3390/ijerph19084556
- Huang, Y., Xu, Z., Huang, Y., Ma, D., Yang, J., and Mays, J. W. (2003). Characterization of poly(ε-caprolactone) via size exclusion Chromatography with online right-angle laser-light scattering and viscometric detectors. *Int. J. Polym. Anal. Charact.* 8, 383–394. doi:10.1080/714975019
- Huda, M. S., Drzal, L. T., Mohanty, A. K., and Misra, M. (2005). Wood-fiber-reinforced poly(lactic acid) composites: evaluation of the physicomechanical and morphological properties. *Wood Fiber Reinf. Poly (Lact. Acid.) Compos.* 102, 4856–4869. doi:10.1002/app.24829
- Huitric, J., Ville, J., Médéric, P., Moan, M., and Aubry, T. (2009). Rheological, morphological and structural properties of PE/PA/nanoclay ternary blends: effect of clay weight fraction. *J. Rheol.* 53 (5), 1101–1119. doi:10.1122/1.3153551
- Huneault, M. A., and Li, H. (2012). Preparation and properties of extruded thermoplastic starch/polymer blends. *J. Appl. Polym. Sci.* 126, 1–13. doi:10.1002/app.36724
- Jacobs, U., Fahrlander, M., Winterhalter, J., and Friedrich, C. (1999). Analysis of Palierne's emulsion model in the case of viscoelastic interfacial properties. *J. Rheol. (N. Y. N. Y.)* 43 (6), 1495–1509. doi:10.1122/1.551056
- Javadzadeh, M., Arefazar, A., and Zakizadeh, M. (2020). The effect of glycidyl methacrylate and styrene comonomers on compatibility, physical-mechanical properties, and swelling behavior of SBR/NBR blends. *Polym. Eng. Sci.* 60, 1278–1290. doi:10.1002/pen.25379
- Jha, N. S., Rathod, P., Wagh, S. M., and Pande, S. A. (2019). Investigation on the mechanical, thermal properties of polyamide 6/polypropylene blends with natural talc as filler. *AIP Conf. Proc.* 2104 (1), 1–10.
- Juntuek, P., Ruksakulpiwat, C., Chumsamrong, P., and Ruksakulpiwat, Y. (2012). Effect of glycidyl methacrylate-grafted natural rubber on physical properties of polylactic acid and natural rubber blends. *Appl. Polym. Sci.* 125, 745–754. doi:10.1002/app.36263
- Koivula, H., Toivakka, M., and Gane, P. (2012). Short time spreading and wetting of offset printing liquids on model calcium carbonate coating structures. *J. Colloid Interface Sci.* 369, 426–434. doi:10.1016/j.jcis.2011.11.065
- Kong, Y., Qian, S., Zhang, Z., Cheng, H., and Liu, Y. (2023). Constructing stable 'bridge' structures with compatibilizer POE-g-GMA to improve the compatibility of starch-based composites. *Polym. Eng. Sci.* 63 (4), 1106–1115. doi:10.1002/pen.26267
- Kumar, M., Mohanty, S., Nayak, S. K., and Rahail Parvaiz, M. (2010). Effect of glycidyl methacrylate (GMA) on the thermal, mechanical and morphological property of biodegradable PLA/PBAT blend and its nanocomposites. *Bioresour. Technol.* 101, 8406–8415. doi:10.1016/j.biortech.2010.05.075

- Lacroix, C., and Carreau, P. J. (1997). Linear viscoelastic behavior of molten polymer blends: a comparative study of the Palierne and Lee and Park models. *Rheol. Acta* 36, 416–428. doi:10.1007/s003970050057
- Li, H., and Huneault, M. A. (2011). Effect of chain extension on the properties of PLA/TPS blends. *Appl. Polym. Sci.* 122, 134–141. doi:10.1002/app.33981
- Liang, J. Z., Duan, D. R., Tang, C. Y., Tsui, C. P., Chen, D. Z., and Zhang, S. D. (2015). Mechanical properties and morphology of poly(L-lactic acid)/Nano-CaCO₃ composites. *J. Polym. Env.* 23, 21–29. doi:10.1007/s10924-014-0661-z
- Liao, H., Li, S., Liu, C., and Tao, G. (2020). Rheological investigation with palierne's model on a polystyrene/nylon 6 blending melt compatibilized by a polystyrene grafted maleic anhydride. *Open J. Org. Polym. Mater.* 10, 17–25. doi:10.4236/ojopm.2020.102002
- Lim, L. T., Auras, R., and Rubino, M. (2008). Processing technologies for poly(lactic acid). *Prog. Polym. Sci.* 33, 820–852. doi:10.1016/j.progpolymsci.2008.05.004
- Liu, Z., Liu, W., Ma, L., Mo, M., Huang, Y., Lai, W., et al. (2024). Effect of inorganic particles gradation on the properties of high-filled unsaturated polyester resin/CaCO₃ composites. *Polym. Compos.* 45 (2), 1494–1507. doi:10.1002/pc.27869
- Maglio, G., Malinconico, M., Migliozzi, A., and Groeninckx, G. (2004). Immiscible poly(L-lactide)/poly(ϵ -caprolactone) blends: influence of the addition of a poly(L-lactide)-poly(oxyethylene) block copolymer on thermal behavior and morphology. *Macromol. Chem. Phys.* 205, 946–950. doi:10.1002/macp.200300150
- Matumba, K. I., Motloung, M. P., Ojijo, V., Ray, S. S., and Sadiku, E. R. (2023). Investigation of the effects of chain extender on material properties of PLA/PCL and PLA/PEG blends: comparative study between polycaprolactone and polyethylene glycol. *Polym. (Basel)* 15 (2230), 2230. doi:10.3390/polym15092230
- Na, Y., He, Y., Shuai, X., Kikkawa, Y., Doi, Y., and Inoue, Y. (2002). Compatibilization effect of poly (caprolactone) -b-poly (ethylene glycol) block copolymers and phase morphology analysis in immiscible poly (lactide)/poly (caprolactone) blends. *Biomacromolecules* 3, 1179–1186. doi:10.1021/bm020050r
- Najafi, N., Heuzey, M. C., and Carreau, P. J. (2012). Poly(lactide) (PLA) -clay nanocomposites prepared by melt compounding in the presence of a chain extender. *Compos. Sci. Technol.* 72, 608–615. doi:10.1016/j.compscitech.2012.01.005
- Najafi, N., Heuzey, M. C., and Carreau, P. J. (2013). Crystallization behavior and morphology of poly(lactide) and PLA/clay nanocomposites in the presence of chain extenders. *Polym. Eng. Sci.* 53, 1053–1064. doi:10.1002/pen.23355
- Oksman, K., Mathew, A. P., Bondeson, D., and Kvien, I. (2006). Manufacturing process of cellulose whiskers/poly(lactic acid) nanocomposites. *Compos. Sci. Technol.* 66, 2776–2784. doi:10.1016/j.compscitech.2006.03.002
- Özen Öner, E., Pekdemir, M. E., Ercan, E., Say, Y., Kök, M., and Aydoğdu, Y. (2022). Novel of (PLA/PCL blend)/Gd₂O₃ rare earth oxide nanocomposites: shape memory effect, thermal, magnetic, and mechanical properties. *Polym. Compos.* 43, 3096–3103. doi:10.1002/pc.26602
- Palade, L. I., Lehermeier, H. J., and Dorgan, J. R. (2001). Melt rheology of high L-content poly(lactic acid). *Macromolecules* 34, 1384–1390. doi:10.1021/ma001173b
- Pasanphan, W., Haema, K., Kongkaoropham, P., Phongtamrug, S., and Piroonpan, T. (2021). Glycidyl methacrylate functionalized star-shaped polylactide for electron beam modification of poly(lactic acid): synthesis, irradiation effects and microwave-resistant studies. *Polym. Degrad. Stab.* 189, 109619. doi:10.1016/j.polymdegradstab.2021.109619
- Pilla, S., Kim, S. G., Auer, G. K., Gong, S., and Park, C. B. (2009). Microcellular extrusion-foaming of poly(lactide) with chain-extender. *Polym. Eng. Sci.* 46, 1653–1660. doi:10.1002/pen.21385
- Qader, I. N., Pekdemir, M. E., Coşkun, M., Kanca, M. S., Kök, M., and Dağdelen, F. (2022). Biocompatible PLA/PCL blends nanocomposites doped with nanographite: physico-chemical, and thermal behaviour. *J. Polym. Res.* 29 (264), 264. doi:10.1007/s10965-022-03117-z
- Rocha, D. B., de Souza, A. G., Szostak, M., and Rosa, D. dos S. (2020). Poly(lactic acid)/Lignocellulosic residue composites compatibilized through a starch coating. *Polym. Compos.* 41 (8), 3250–3259. doi:10.1002/pc.25616
- Rodríguez, L., Arraiza, L., Meaurio, E., and Sarasua, J. (2006). Crystallization, morphology, and mechanical behavior of poly(lactide)/poly (caprolactone) blends. *Polym. Eng. Sci.* 46, 1299–1308. doi:10.1002/pen.20609
- Sabzi, M., Jiang, L., Liu, F., Ghasemi, I., and Atai, M. (2013). Graphene nanoplatelets as poly(lactic acid) modifier: linear rheological behavior and electrical conductivity. *Mater. Chem. A* 1, 8253–8261. doi:10.1039/c3ta11021d
- Salehiyan, R., Yusuuf, A. A., Hassan, A., and Akbari, A. (2015). Poly(lactic acid)/polycaprolactone nanocomposite: influence of montmorillonite and impact modifier on mechanical, thermal, and morphological properties. *Elastomers Plast.* 47 (1), 69–87. doi:10.1177/0095244313489906
- Semba, T., Kitagawa, K., Ishiaku, U. S., and Hamada, H. (2006). The effect of crosslinking on the mechanical properties of poly(lactic acid)/polycaprolactone blends. *Appl. Polym. Sci.* 101, 1816–1825. doi:10.1002/app.23589
- Shi, Q., Chen, C., Gao, L., Jiao, L., Xu, H., and Guo, W. (2011). Physical and degradation properties of binary or ternary blends composed of poly (lactic acid), thermoplastic starch and GMA grafted POE. *Polym. Degrad. Stab.* 96 (1), 175–182. doi:10.1016/j.polymdegradstab.2010.10.002
- Standau, T., Zhao, C., Castellón, S. M., Bonten, C., and Altstädt, V. (2019). Chemical modification and foam processing of polylactide (PLA). *Polym. (Basel)* 11 (306), 2–39. doi:10.3390/polym11020306
- Sugih, A. K., Drijfhout, J. P., Picchioni, F., Janssen, L. P. B. M., and Heeres, H. J. (2009). Synthesis and properties of reactive interfacial agents for polycaprolactone-starch blends. *Appl. Polym. Sci.* 114, 2315–2326. doi:10.1002/app.30712
- Tábi, T., Sajó, I. E., Szabó, F., Luyt, A. S., and Kovács, J. G. (2010). Crystalline structure of annealed polylactic acid and its relation to processing. *eXPRESS Polym. Lett.* 4 (10), 659–668. doi:10.3144/expresspolymlett.2010.80
- Tham, M. W., Nurul Fazita, M. R., Abdul Khalil, H. P. S., Jaafar, M., Rashedi, A., and Mohamad Haafiz, M. K. (2022). Biocomposites based on poly(lactic acid) matrix and reinforced with natural fiber fabrics: the effect of fiber type and compatibilizer content. *Polym. Compos.* 43, 4191–4209. doi:10.1002/pc.26681
- Todo, M., and Takayam, T. (2011). Fracture mechanisms of biodegradable PLA and PLA/PCL blends. *Biomater. - Phys. Chem.*, 374–393.
- Torres, E., Gaona, A., García-Bosch, N., Muñoz, M., Fombuena, V., Moriana, R., et al. (2021). Improved mechanical, thermal, and hydrophobic properties of PLA modified with alkoxy silanes by reactive extrusion process. *Polym. (Basel)* 13 (2475), 2475. doi:10.3390/polym13152475
- Tuancharoensri, N., Ross, G. M., Kongprayoon, A., Mahasaronon, S., Pratumshat, S., Viyoch, J., et al. (2023). *In situ* compatibilized blends of PLA/PCL/CAB melt-blown films with high elongation: investigation of miscibility, morphology, crystallinity and modelling. *Polym. (Basel)* 15 (303), 303–320. doi:10.3390/polym15020303
- Vermant, J., Cioccolo, G., Golapan Nair, K., and Moldenaers, P. (2004). Coalescence suppression in model immiscible polymer blends by nano-sized colloidal particles. *Rheol. Acta* 43, 529–538. doi:10.1007/s00397-004-0381-8
- Vignati, E., Piazza, R., and Lockhart, T. P. (2003). Pickering emulsions: interfacial tension, colloidal layer morphology, and trapped-particle motion. *Langmuir* 19, 6650–6656. doi:10.1021/la034264l
- Vinckier, I., Mewis, J., and Moldenaers, P. (1999b). Elastic recovery of immiscible blends Part 2: transient flow histories. *Rheol. Acta* 38, 198–205. doi:10.1007/s003970050169
- Vinckier, I., Moldenaers, P., and Mewis, J. (1999a). Elastic recovery of immiscible blends 1. Analysis after steady state shear flow. *Rheol. Acta* 38, 65–72. doi:10.1007/s003970050156
- Wagener, R., and Reisinger, T. J. G. (2003). A rheological method to compare the degree of exfoliation of nanocomposites. *Polym. Guildf.* 44, 7513–7518. doi:10.1016/j.polymer.2003.01.001
- Xu, X., Lifeng Ma, C. L., and Liu, C. (2022). Bio-based poly(lactic acid) or epoxy natural rubber thermoplastic vulcanizates with dual interfacial compatibilization networks. *Polym. Eng. Sci.* 62 (6), 1987–1998. doi:10.1002/pen.25981
- Ye, G., Gu, T., Chen, B., Bi, H., and Hu, Y. (2023). Mechanical, thermal properties and shape memory behaviors of PLA/PCL/PLA-g-GMA blends. *Polym. Eng. Sci.* 63 (7), 2084–2092. doi:10.1002/pen.26347
- Ye, G., Li, Z., Chen, B., Bai, X., Chen, X., and Hu, Y. (2022). Performance of poly(lactic acid)/polycaprolactone/microcrystalline cellulose biocomposites with different filler contents and maleic anhydride compatibilization. *Polym. Compos.* 43, 5179–5188. doi:10.1002/pc.26807
- Yeh, J., Wu, C., Tsou, C., Chai, W. L., Chow, J. D., Huang, C. Y., et al. (2009). Study on the crystallization, miscibility, morphology, properties of poly (lactic acid)/poly (caprolactone) blends. *Polym. Plast. Technol. Eng.* 48, 571–578. doi:10.1080/03602550902824390
- Zachariah, A. K., Geethamma, V. G., Chandra, A. K., Mohammed, P. K., and Thomas, S. (2014). Rheological behaviour of clay incorporated natural rubber and chlorobutyl rubber nanocomposites. *R. Soc. Chem.* 101.
- Zhai, S., Liu, Q., Zhao, Y., Sun, H., Yang, B., and Weng, Y. (2021). A review: research progress in modification of poly (lactic acid) by lignin and cellulose. *Polym. (Basel)* 13 (3), 38–44. doi:10.3390/polym13050776
- Zhang, N., Wang, Q., Ren, J., and Wang, L. (2009). Preparation and properties of biodegradable poly(lactic acid)/poly(butylene adipate-co-terephthalate) blend with glycidyl methacrylate as reactive processing agent. *J. Mater. Sci.* 44, 250–256. doi:10.1007/s10853-008-3049-4
- Zhou, Z. F., Huang, G. Q., Xu, W. B., and Ren, F. M. (2007). Chain extension and branching of poly(L-lactic acid) produced by reaction with a DGEBA-based epoxy resin. *Express Polym. Lett.* 1 (11), 734–739. doi:10.3144/expresspolymlett.2007.101